Cavity-assisted spontaneous emission of a single Λ-type emitter as a source of single-photon packets with controlled shape

M. Khanbekyan*
Institut für Theoretische Physik, Universität Magdeburg, Postfach 4120, D-39016 Magdeburg, Germany

D.-G. Welsch
Theoretisch-Physikalisches Institut, Friedrich-Schiller-Universität Jena, Max-Wien-Platz 1, D-07743 Jena, Germany
(Dated: January 5, 2017)

The radiation emitted by a classically pumped three-level Λ-type emitter in a resonator cavity featuring both radiative and unwanted losses is studied. In particular, the efficiency of one-photon Fock state excitation of the outgoing wave packet and the spatiotemporal shape of the wave packet are investigated. It is shown that for given shape of the emitter–cavity interaction, adjusting the shape of the pump pulse renders it possible to generate the emission of one-photon Fock state wave packets of desired shape with high efficiency.

arXiv:1701.00984v1 [quant-ph] 4 Jan 2017

I. INTRODUCTION

The interaction of a single emitter with the quantized radiation-field in a high-Q cavity serves as a basic ingredient in various schemes in quantum information science (for a review see, e. g., Ref. [1]). In this context, an essential prerequisite for quantum information processing [2] is the deterministic generation of indistinguishable light pulses of one-photon Fock states on demand with well-controlled features, such as efficiency, frequency, polarization, timing etc.. Among the various features of single-photon emission, control and manipulation of the spatiotemporal shape of the single-photon light pulses is essential for quantum network applications where symmetric wavepackets are required for a time reversal of the emission process [3] or where time-bin entanglement is used [4].

The most prominent way to generate single-photon Fock states in high-finesse optical cavities interacting with single emitters is based on vacuum stimulated Raman adiabatic approach (vSTIRAP) technique [5, 6]. A single transition of an emitter with a Λ-type energy level scheme is excited by a pump laser stimulating the emission into a strongly coupled cavity–emitter transition. Alongside the principal realizations of vSTIRAP in atomic systems (see e.g. [7]), a Λ-type scheme can be also implemented in semiconductor quantum dot–microcavity systems, where a Λ-type system is created by applying a strong magnetic field to a singly charged quantum dot resulting in Zeeman splitting of the spin states in the conduction band [8] or by applying a lateral electric field which charges a single quantum dot with a single electron resulting in optical transitions between ground and excited electron states and the charged exciton [9]. In particular, in atomic systems control of the photon frequency [10], wavepacket length [10] and phase [7] have been reported. The efficiency of the generation of single-photon Fock states in a scheme based on vSTIRAP technique is governed by an interplay of various system parameters, such as the transition dipole matrix element, intensity and amplitude of the pump pulse, frequency detuning etc. Further, it has also been reported that the spatiotemporal shapes of the outgoing wave packets of the emitted one-photon Fock state radiation follow the driving laser pulse shapes [11, 12]. However, this behavior is only observed for a certain range of parameters and the efficiency of one-photon Fock state generation is very low, which makes it impossible to use the scheme for further applications in quantum communications. More recently, the possibility of generation of single-photon wave packets with arbitrary shapes in the case when the atom–cavity interaction remains constant during the generation process has been demonstrated both theoretically, on using the master equation formalism for describing the atom–photon system [13], and experimentally, with un-trapped atoms injected into a cavity by means of an atomic fountain [14].

In an earlier work, we have studied the potential of a single two-level atom in a high-Q cavity as a single-photon emitter, where the wave packet associated with the emitted photon is shorter than the cavity decay time [15, 16]. Within the frame of exact quantum electrodynamics, we have particularly shown the feasibility of the generation of single-photon wave packets with time-symmetric spatiotemporal shapes.

In the present article we extend the theory to the interaction of a pumped three-level Λ-type emitter with a realistic cavity-assisted quantized electromagnetic field, with the aim of well-defined and controlled one-photon Fock-state emission. In particular, we study in detail both the properties of the excited outgoing wave packet and the efficiency to prepare it in a single-photon Fock state. The general explicit expression derived for the spatiotemporal shape of the excited outgoing wave packet allows us to study different coupling regimes of the emitter–pump and the emitter–cavity-field interactions. In this context, we show the possibility to generate single-photon wave packets with requested spatiotemporal shapes, which can be

*E-mail address: mikayel.khanbekyan@ovgu.de

achieved by using appropriately designed driving laser pulses.

The paper is organized as follows. The basic equations for the resonant interaction of an emitter with a cavity-assisted electromagnetic field are given in Sec. II. In Sec. III the Wigner function of the quantum state the excited outgoing wave packet is prepared in and the spatiotemporal shape of the wave packet are studied for the case of a classically pumped three-level Λ-type emitter. Section IV is devoted to the problem of generating single-photon wave packets of desired shapes. A summary and some concluding remarks are given in Sec. V.

II. BASIC EQUATIONS

We consider a single emitter (position $\mathbf{r}_A$) that interacts with the electromagnetic field in the presence of a dispersing and absorbing dielectric medium with a spatially varying and frequency-dependent complex permittivity

$$\varepsilon(\mathbf{r},\omega) = \varepsilon'(\mathbf{r},\omega) + i\varepsilon''(\mathbf{r},\omega), \tag{1}$$

with the real and imaginary parts $\varepsilon'(\mathbf{r},\omega)$ and $\varepsilon''(\mathbf{r},\omega)$, respectively. Applying the multipolar-coupling scheme in electric dipole approximation, we may write the Hamiltonian that governs the temporal evolution of the overall system, which consists of the electromagnetic field, the dielectric medium (including the dissipative degrees of freedom), and the emitter coupled to the field, in the form of (for details, see Refs. [17, 18])

$$\hat{H} = \int \mathrm{d}^3 r \int_0^\infty \mathrm{d}\omega\, \hbar\omega\, \hat{\mathbf{f}}^\dagger(\mathbf{r},\omega)\cdot\hat{\mathbf{f}}(\mathbf{r},\omega) + \sum_k \hbar\omega_{kk}\hat{S}_{kk} - \hat{\mathbf{d}}_A\cdot\hat{\mathbf{E}}(\mathbf{r}_A). \tag{2}$$

In this equation, the first term is the Hamiltonian of the field–medium system, where the fundamental bosonic fields $\hat{\mathbf{f}}(\mathbf{r},\omega)$ and $\hat{\mathbf{f}}^\dagger(\mathbf{r},\omega)$,

$$\big[\hat{\mathbf{f}}(\mathbf{r},\omega), \hat{\mathbf{f}}^\dagger(\mathbf{r}',\omega')\big] = \delta(\omega-\omega')\boldsymbol{\delta}(\mathbf{r}-\mathbf{r}'), \tag{3}$$

$$\big[\hat{\mathbf{f}}(\mathbf{r},\omega), \hat{\mathbf{f}}(\mathbf{r}',\omega')\big] = \mathbf{0}, \tag{4}$$

play the role of the canonically conjugate system variables. The second term is the Hamiltonian of the emitter, where the $\hat{S}_{kk'}$ are the flip operators,

$$\hat{S}_{kk'} = |k\rangle\langle k'|, \tag{5}$$

corresponding to the $|k\rangle \leftrightarrow |k'\rangle$ transition with the frequency $\omega_{kk'}$, where $|k\rangle$ is the energy eigenstates of the emitter. Finally, the last term is the emitter–field coupling energy, where

$$\hat{\mathbf{d}}_A = \sum_{kk'} \mathbf{d}_{Akk'}\hat{S}_{kk'} \tag{6}$$

is the electric dipole-moment operator ($\mathbf{d}_{Akk'} = \langle k|\hat{\mathbf{d}}_A|k'\rangle$), and the operator of the medium-assisted electric field $\hat{\mathbf{E}}(\mathbf{r})$ can be expressed in terms of the variables $\hat{\mathbf{f}}(\mathbf{r},\omega)$ and $\hat{\mathbf{f}}^\dagger(\mathbf{r},\omega)$ as follows:

$$\hat{\mathbf{E}}(\mathbf{r}) = \hat{\mathbf{E}}^{(+)}(\mathbf{r}) + \hat{\mathbf{E}}^{(-)}(\mathbf{r}), \tag{7}$$

$$\hat{\mathbf{E}}^{(+)}(\mathbf{r}) = \int_0^\infty \mathrm{d}\omega\, \underline{\hat{\mathbf{E}}}(\mathbf{r},\omega), \quad \hat{\mathbf{E}}^{(-)}(\mathbf{r}) = [\hat{\mathbf{E}}^{(+)}(\mathbf{r})]^\dagger, \tag{8}$$

$$\underline{\hat{\mathbf{E}}}(\mathbf{r},\omega) = i\sqrt{\frac{\hbar}{\varepsilon_0\pi}}\,\frac{\omega^2}{c^2}\int \mathrm{d}^3 r' \sqrt{\varepsilon''(\mathbf{r}',\omega)}\,\mathsf{G}(\mathbf{r},\mathbf{r}',\omega)\cdot\hat{\mathbf{f}}(\mathbf{r}',\omega). \tag{9}$$

In the above, the classical (retarded) Green tensor $\mathsf{G}(\mathbf{r},\mathbf{r}',\omega)$ is the solution to the equation

$$\boldsymbol{\nabla}\times\boldsymbol{\nabla}\times\mathsf{G}(\mathbf{r},\mathbf{r}',\omega) - \frac{\omega^2}{c^2}\,\varepsilon(\mathbf{r},\omega)\mathsf{G}(\mathbf{r},\mathbf{r}',\omega) = \boldsymbol{\delta}^{(3)}(\mathbf{r}-\mathbf{r}') \tag{10}$$

together with the boundary condition at infinity, $\mathsf{G}(\mathbf{r},\mathbf{r}',\omega)\to 0$ if $|\mathbf{r}-\mathbf{r}'|\to\infty$, and defines the structure of the electromagnetic field formed by the present dielectric bodies.

III. SINGLE-PHOTON GENERATION EFFICIENCY AND WAVE PACKET SHAPE

A. Pumped three-level Λ-type emitter in a cavity

Let us consider a single atom-like emitter placed in a resonator cavity and assume that only a single transition ($|2\rangle \leftrightarrow |3\rangle$, frequency ω_{23}) is quasi resonantly coupled to a narrow-band cavity-assisted electromagnetic field (frequency ω_k), cf. Fig. 1. We further assume, that an external (classical) pump field with quasi resonant frequency ω_p and (time-dependent) Rabi frequency $\Omega_p(t)$ is applied to the $|1\rangle \leftrightarrow |2\rangle$ transition (frequency ω_{21}), cf. Fig. 1. For the sake of simplicity of presentation, we restrict our treatment to the one-dimensional case (z axis) and assume that the resonator cavity is formed by an empty body bounded by an outcoupling fractionally transparent mirror at $z=0$ and a perfectly reflecting mirror at $z=-l$, and (negative) z_A is the position of the emitter inside the cavity.

In this case, the one-dimensional version of the Hamiltonian (2) in the rotating-wave approximation reads

$$\hat{H} = \int \mathrm{d}z \int_0^\infty \mathrm{d}\omega \hbar\omega \hat{f}^\dagger(z,\omega)\hat{f}(z,\omega) + \hbar\omega_{21}\hat{S}_{22} + \hbar\omega_{31}\hat{S}_{33} - g(t)\left[d_{23}\hat{S}_{32}^\dagger\hat{E}^{(+)}(z_A) + \text{H.c.}\right] - \frac{\hbar}{2}\Omega_p(t)\left[\hat{S}_{12}^\dagger e^{-i\omega_p t} + \text{H.c.}\right], \tag{11}$$

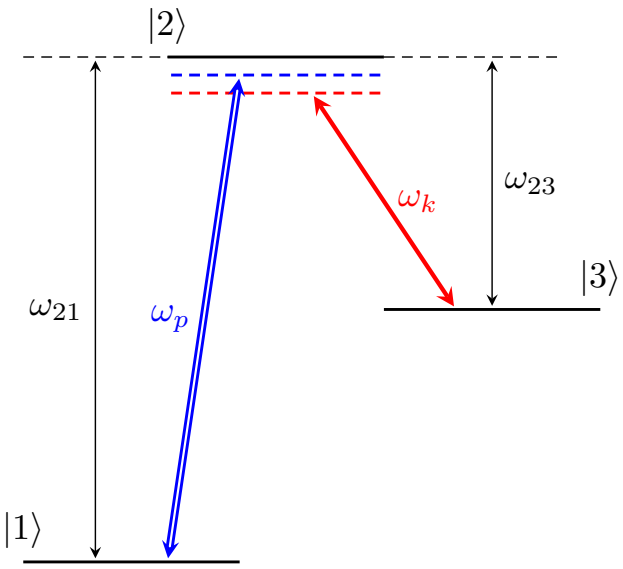

FIG. 1: Scheme of energy levels and transitions for the three-level Λ-type atomic emitter.

with $\omega_{31}=\omega_{21}-\omega_{23}$. Here, the (real) time-dependent function $g(t)$ defines the (time-dependent) shape of the interaction of the emitter with the cavity field, which without loss of generality can be chosen to be normalized to unity. It may be used to simulate the (quasistatic) motion of the emitter through the cavity in the direction perpendicular to the cavity axis and/or motion along the cavity axis.

In what follows we assume that the emitter is initially (at time $t=0$) prepared in the state $|1\rangle$ and the rest of the system, i. e., the part of the system that consists of the electromagnetic field and the dielectric media (i. e., the cavity), is prepared in the ground state $|\{0\}\rangle$. Since, in the case under consideration, we may approximately span the Hilbert space of the whole system by the single-excitation states, we may expand the state vector of the overall system at later times t ($t\geq 0$) as

$$|\psi(t)\rangle = C_1(t)|\{0\}\rangle|1\rangle + C_2(t)e^{-i\omega_{21}t}|\{0\}\rangle|2\rangle + \int \mathrm{d}z \int_0^\infty \mathrm{d}\omega\, C_3(z,\omega,t)e^{-i(\omega+\omega_{31})t}\hat{f}^\dagger(z,\omega)|\{0\}\rangle|3\rangle, \tag{12}$$

where $\hat{f}^\dagger(z,\omega)|\{0\}\rangle$ is an excited single-quantum state of the combined field–cavity system.

It is not difficult to prove that the Schrödinger equation for $|\psi(t)\rangle$ leads to the following system of differential equations for the probability amplitudes $C_1(t)$, $C_2(t)$ and $C_3(z,\omega,t)$:

$$\dot{C}_1 = \frac{i}{2}\Omega_p(t)e^{i\Delta_p t}C_2(t), \tag{13}$$

$$\dot{C}_2 = \frac{i}{2}\Omega_p(t)e^{-i\Delta_p t}C_1(t) - \frac{d_{23}}{\sqrt{\pi\hbar\varepsilon_0\mathcal{A}}}\int_0^\infty \mathrm{d}\omega\,\frac{\omega^2}{c^2}\int \mathrm{d}z\sqrt{\varepsilon''(z,\omega)} \times G(z_A,z,\omega)C_3(z,\omega,t)g(t)e^{-i(\omega-\omega_{23})t}, \tag{14}$$

$$\dot{C}_3(z,\omega,t) = \frac{d_{23}^*}{\sqrt{\pi\hbar\varepsilon_0\mathcal{A}}}\frac{\omega^2}{c^2}\sqrt{\varepsilon''(z,\omega)} \times G^*(z_A,z,\omega)C_2(t)g(t)e^{i(\omega-\omega_{23})t}, \tag{15}$$

where $\mathcal{A}$ is the area of the coupling mirror of the cavity, and $\Delta_p=\omega_p-\omega_{21}$ is the detuning of the pump frequency from the $|1\rangle\leftrightarrow|2\rangle$ transition frequency. The Green function $G(z,z',\omega)$ determines the spectral response of the resonator cavity. For a sufficiently high-Q cavity, the excitation spectrum effectively turns into a quasi-discrete set of lines of mid-frequencies ω_k and widths Γ_k, according to the poles of the Green function at the complex frequencies

$$\tilde{\omega}_k = \omega_k - \tfrac{1}{2}i\Gamma_k, \tag{16}$$

where the linewidths are much smaller than the line separations,

$$\Gamma_k \ll \tfrac{1}{2}(\omega_{k+1}-\omega_{k-1}). \tag{17}$$

In this case, assuming that the kth mode of the cavity is quasi resonantly coupled to the transition $|2\rangle\leftrightarrow|3\rangle$ with the transition frequency ω_{23} (cf. Fig. 1), we substitute the formal solutions to Eqs. (13) and (15) [with the initial condition $C_1(0)=1$, $C_2(0)=0$ and $C_3(z,\omega,0)=0$] into Eq. (14). Then, using the relations for the Green tensor $G(z_1,z_2,\omega)$ as given by Eqs. (A1) and (A2), we can derive the integro-differential equation

$$\dot{C}_2 = \frac{i}{2}\Omega_p(t)e^{-i\Delta_p t} + \int_0^t \mathrm{d}t'\,K(t,t')C_2(t'), \tag{18}$$

where the kernel function $K(t,t')$ reads

$$K(t,t') = -\frac{1}{4}\Omega_p(t)\Omega_p(t')e^{-i\Delta_p(t-t')} - \frac{1}{4}\alpha_k\tilde{\omega}_k g(t)g(t')e^{-i(\Delta_k-i\Gamma_k/2)(t-t')}, \tag{19}$$

with $\Delta_k=\omega_k-\omega_{23}$ and

$$\alpha_k = \frac{4|d_{23}|^2}{\hbar\varepsilon_0\mathcal{A}l}\sin^2(\omega_k z_A/c). \tag{20}$$

From Eq. (18) together with Eq. (19) we can conclude that $R_k\equiv\sqrt{\alpha_k\omega_k}$ can be regarded as vacuum Rabi frequency of emitter–cavity interaction.

Following Ref. [15], it can be shown that when the Hilbert space of the system is effectively spanned by a single excitation, on a time-scale that is short compared

to the inverse spontaneous emission rate of the emitter, the multimode Wigner function of the quantum state of the outgoing field can be derived to be (Appendix B)

$$W_{\rm out}(\alpha_i,t) = W_1(\alpha_1,t)\prod_{i\neq 1} W_i^{(0)}(\alpha_i,t), \qquad (21)$$

where

$$W_1(\alpha,t) = [1-\eta(t)]W_1^{(0)}(\alpha) + \eta(t)W_1^{(1)}(\alpha), \qquad (22)$$

with $W_i^{(0)}(\alpha)$ and $W_i^{(1)}(\alpha)$ being the Wigner functions of the vacuum state and the one-photon Fock state, respectively, for the ith nonmonochromatic mode. As we see, the mode labeled by the subscript $i=1$, is basically prepared in a mixed state of a one-photon Fock state and the vacuum state, due to unavoidable existence of unwanted losses. The other nonmonochromatic modes of the outgoing field with $i\neq 1$ are in the vacuum state and, therefore, remain unexcited.

The Wigner function $W_1(\alpha,t)$ of the mode associated with the excited outgoing wave packet reveals that $\eta(t)$ can be regarded as being the efficiency to prepare the excited outgoing wave packet in a one-photon Fock state (Appendix B):

$$\eta(t) = \int_0^\infty {\rm d}\omega\, |F(\omega,t)|^2 \simeq \int_{-\infty}^\infty {\rm d}\omega\, |F(\omega,t)|^2, \qquad (23)$$

with

$$F(\omega,t) = \frac{d_{23}}{\sqrt{\pi\hbar\varepsilon_0\mathcal{A}}}\sqrt{\frac{c}{\omega}}\frac{\omega^2}{c^2}$$
$$\times\int_0^t {\rm d}t' G^*(0^+,z_A,\omega)C_2^*(t')g(t')e^{i\omega(t-t')}e^{i\omega_{23}t'}e^{i\omega_{31}t}, \qquad (24)$$

where 0^+ indicates the position $z=0$ outside the cavity. The excited outgoing wave packet (mid-frequency ω_k) is characterized by the mode function

$$F_1(\omega,t) = \frac{F(\omega,t)}{\sqrt{\eta(t)}}\,. \qquad (25)$$

The intensity of the outgoing field at position z is given by

$$I(z,t) = \eta(t)|\phi_1(z,t)|^2, \qquad (26)$$

with

$$\phi_1(z,t) = \frac{1}{2}\int_0^\infty {\rm d}\omega \sqrt{\frac{\hbar\omega}{\varepsilon_0 c\pi\mathcal{A}}}\, e^{-i\omega z/c}F_1(\omega,t). \qquad (27)$$

Equation (26) reveals that $\phi_1(z,t)$ represents the spatiotemporal shape of the outgoing field associated with the excited nonmonochromatic mode $F_1(\omega,t)$.

B. Efficiency of single-photon Fock state generation

Inserting Eq. (24) into Eq. (23) and using Eq. (A3), we find the efficiency of one-photon Fock state generation as

$$\eta(t) = \frac{R_k^2}{4}\frac{\gamma_{k\rm rad}}{\Gamma}\Big[\int_0^t {\rm d}t'\, g(t')C_2(t')$$
$$\times\int_0^{t'} {\rm d}t''\, g(t'')C_2^*(t'')e^{i(\Delta_k+i\Gamma_k/2)(t'-t'')} + {\rm C.c.}\Big], \qquad (28)$$

where $\gamma_{k\rm rad}$ describes the wanted radiative losses due to transmission of the radiation through the fractionally transparent mirror. As we can see, the efficiency is proportional to the ratio $\gamma_{k\rm rad}/\Gamma_k$, where the damping parameter Γ_k can be regarded as being the sum $\Gamma_k = \gamma_{k\rm rad} + \gamma_k'$, where γ_k' describes the unwanted losses due to absorption. For the numerical calculations, we will assume $\gamma_{k\rm rad}/\Gamma_k = 0.9$, which corresponds to 10% unwanted losses. Apart from the unavoidably existing unwanted losses, the one-photon Fock state efficiency depends on the shape $g(t)$ and the Rabi frequency R_k of the emitter–cavity interaction and the shape and the intensity of the external pump field. Finally, inserting Eq. (25) together with Eq. (24) into Eq. (27) and using Eq. (A3), we find the spatiotemporal shape of the excited outgoing wave packet outside the cavity as (in the following, for the sake of simplicity, we assume $\omega_{31}=0$)

$$\phi_1(z,t) = \frac{R_k}{2}\sqrt{\frac{\hbar\omega_k\gamma_{k\rm rad}}{2\varepsilon_0 c\mathcal{A}\eta(t)}}$$
$$\times\int_0^{t-z/c} {\rm d}t'\, C_2^*(t')g(t')e^{-i(\Delta_k+i\Gamma_k/2)t'}\, e^{i\tilde{\omega}_k^*(t-z/c)}. \qquad (29)$$

To present explicit results, we restrict ourselves to times much larger than the time the excited wave packet needs to almost completely exit the cavity. To find the spatiotemporal shape of the excited outgoing wave packet $\phi_1(z,T)$ at time $T\gg\Gamma_k^{-1}$ for given pump intensity and emitter–cavity interaction shapes $\Omega_p(t)$ and $g(t)$, respectively, we first solve Eq. (18) together with Eqs. (19), (20) and the initial condition $C_2(0)=0$. Equation (18) is a Volterra-type integro-differential equation of the second kind, which can be solved using a standard fourth-order Runge-Kutta algorithm. Then, inserting the solution $C_2(t)$ into Eqs. (28) and (29) we can find, respectively, the efficiency of one-photon Fock state emission and the spatiotemporal shape of the wave packet leaving the cavity.

In accordance with the vSTIRAP state-mapping proposal [19, 20], in an ideal system the maximum one-photon Fock state efficiency can be achieved when the dynamics of the system follows the "dark state", which is formed as a superposition of the states $|\{0\}\rangle|1\rangle$ and $\hat{f}^\dagger(z,\omega)|\{0\}\rangle|3\rangle$. This is the case if the process is adiabatic and the emitter–cavity interaction is well-established before the driving pulse is applied. The case

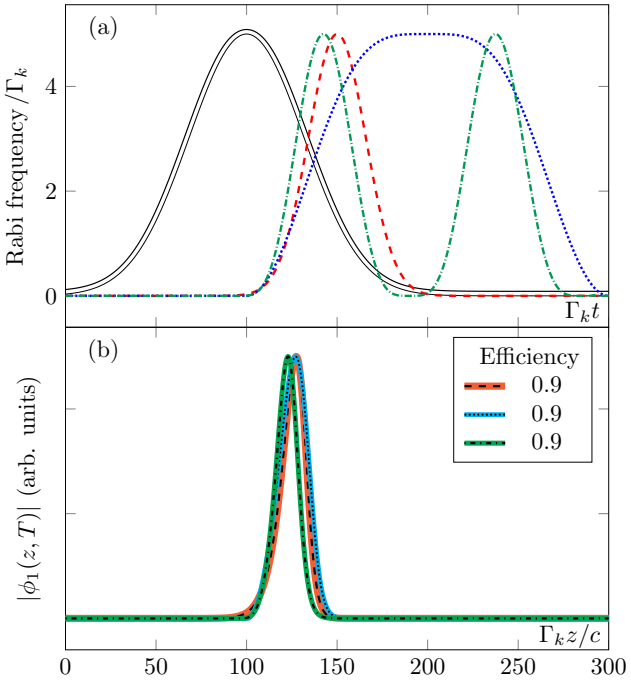

FIG. 2: (a) Various pulse shapes of the pump $\Omega_p(t)$ (dotted, dashed and dash-dotted lines) with the maximum value $\Omega_{p\max} = 5\Gamma_k$ and the shape of the emitter–cavity interaction $g(t)$ (double line, shown as normalized to $\Omega_{p\max}$). (b) Corresponding spatiotemporal shapes of the one-photon Fock state outgoing wave packet ($R_k = 5\Gamma_k$, $\Delta_k = \Delta_p = \Gamma_k$, $T = 350\Gamma_k$).

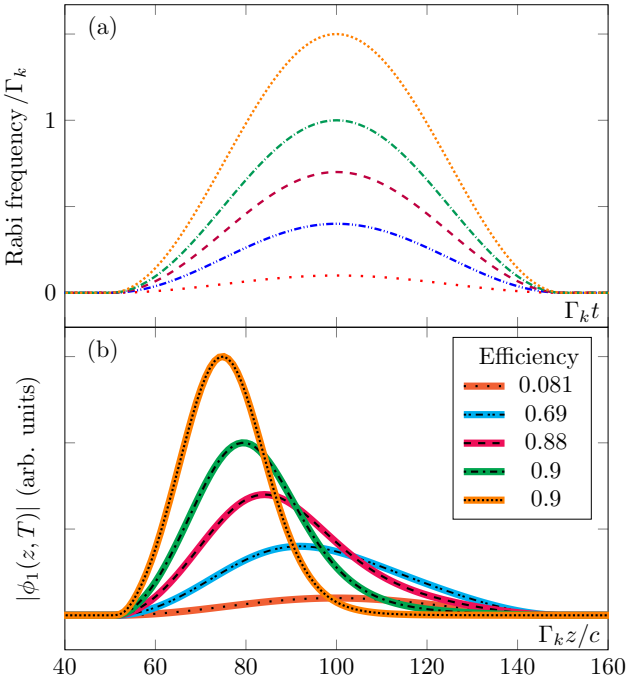

FIG. 3: (a) Various pulse shapes of the pump $\Omega_p(t)$ with the maximum value $\Omega_{p\max} = 0.1\Gamma_k$ (dotted red line), $\Omega_{p\max} = 0.4\Gamma_k$ (dashed-dotted blue line), $\Omega_{p\max} = 0.7\Gamma_k$ (dashed purple line), $\Omega_{p\max} = 1\Gamma_k$ (dashed-dotted green line), $\Omega_{p\max} = 1.5\Gamma_k$ (dotted orange line). (b) Corresponding spatiotemporal shapes of the one-photon Fock state outgoing wave packet ($R_k = 2\Gamma_k$, $\Delta_k = \Delta_p = 0$, $T = 200\Gamma_k$).

of the vSTIRAP is illustrated in Fig. 2, where a Gaussian-type emitter–cavity interaction shape and three driving pulse shapes are considered. Comparing the values of $\eta(T)$, we see that $\eta(T) \approx 0.9$ for all three cases of the driving pulse shapes, which shows that the efficiencies of one-photon Fock state generation is only limited by the unwanted losses in the system. Moreover, Fig. 2 reveals that the excited outgoing wave packet carrying a single photon is generated in the time interval immediately as the driving pulse is applied. Thus, since the adiabatic evolution required by the vSTIRAP is much longer than the cavity mode decay time, the generated single-photon wave packet escapes from the cavity once it is generated, and, hence, the shape of the wave packet $|\phi_1(z,T)|$ is effectively independent of the driving pulse shape.

C. Effects of emitter–cavity and emitter–pump interaction strengths and shapes

In general, it is desirable to have the possibility to control and manipulate the shape of the outgoing wave packet and, at the same time, to excite it in a one-photon Fock state with high efficiency. Let us therefore study the dependencies of the efficiency and the wave packet shape on the emitter–cavity interaction and the emitter–pump interction in more detail. For the sake of transparency we first concentrate on the case, when the emitter–cavity interaction is constant, i.e., it does not vary with time.

In Fig. 3 the spatiotemporal shape of the single-photon outgoing wave packet (solid lines) is shown for various intensities of a symmetric single-peak driving pulse. It is seen that when the value of the maximum of the driving pulse is low, $\Omega_{p\max} = 0.1\Gamma_k$, the shape of the outgoing wave packet (red, solid line in Fig. 3(b)) perfectly coincides with the shape of the driving pulse (red, dotted line in Fig. 3(a)). However, the efficiency of one-photon Fock state generation is quite low, $\eta(T) = 0.081$. It is further seen that the efficiency increases with $\Omega_{p\max}$. On the other hand, the figure also reveals that with increasing $\Omega_{p\max}$ the driving pulse induces the photon emission earlier, and as a result, the shape of the outgoing wave packet does not follow the profile of the driving pulse but features an asymmetric shape.

Next, let us consider the dependence of the spatiotemporal shape of the single-photon outgoing wave packet on the Rabi frequency of the emitter–cavity interaction R_k. In Fig. 4 the shape is plotted for various values of R_k in the case of a symmetric single-peak driving pulse. For $R_k = \Gamma_k$ the vSTIRAP case is seen to be realized, resulting in high-efficiency single-photon Fock state generation and asymmetric spatiotemporal shape of the associated

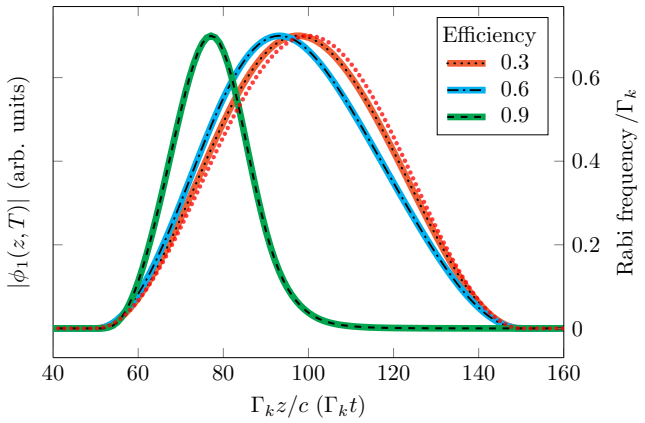

FIG. 4: spatiotemporal shape of the one-photon Fock state outgoing wave packet for $R_k = \Gamma_k$ (solid green line), $R_k = 4\Gamma_k$ (solid blue line), $R_k = 7\Gamma_k$ (solid red line) in the case of a single-peak driving pulse (dotted red line), $\Omega_{p\max} = 0.7\Gamma_k$, $\Delta_k = \Delta_p = 0$, $T = 200\Gamma_k$.

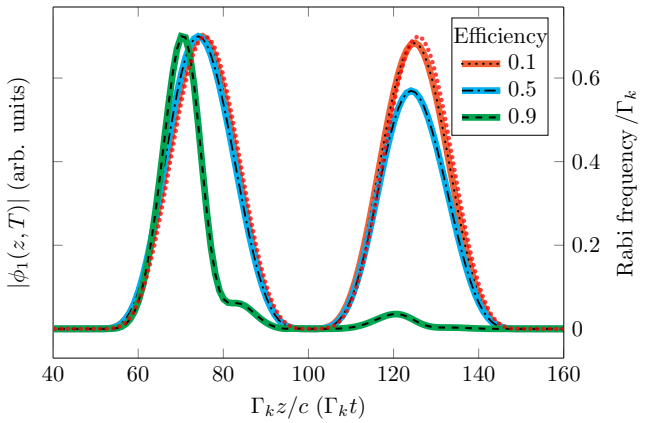

FIG. 5: spatiotemporal shape of the one-photon Fock state outgoing wave packet for $R_k = \Gamma_k$ (solid green line), $R_k = 4\Gamma_k$ (solid blue line), $R_k = 12\Gamma_k$ (solid red line) in the case of a double-peak driving pulse (dotted red line), $\Omega_{p\max} = 0.7\Gamma_k$, $\Delta_k = \Delta_p = 0$, $T = 200\Gamma_k$.

outgoing wave packet. For higher values of R_k, the driving pulse is not strong enough to realize the vSTIRAP, and the efficiency of one-photon Fock state generation is reduced, but the spatiotemporal shape of the associated wave packet follows the shape of the driving pulse.

An analogous situation can be observed for a double-peak driving pulse as illustrated in Fig. 5. For emitter–cavity Rabi frequencies of the same order of magnitude as the driving pulse maximum, the vSTIRAP is again seen to be realized and the efficiency of one-photon Fock state generation is close to the maximum value of 0.9, but the shape of the associated wave packet becomes asymmetric. As expected, for higher rates of emitter–cavity Rabi frequency it follows the driving pulse shape but the one-photon Fock state generation efficiency is rather low.

IV. SHAPE-CONTROLLED SINGLE-PHOTON WAVE PACKET EMISSION

As we have seen, the shape of the single-photon outgoing wave packet can be changed by changing the emitter–cavity interaction and/or the driving pulse. In this context, a question of particular interest is the generation of single-photon wave packets of controlled shapes. To give an answer, let us assume that the desired spatiotemporal shape of the single-photon outgoing wave packet is given by a function $\phi(z,T)$ at some time T, where the condition $T \gg \Gamma_k^{-1}$ again ensures that the wave packet has almost completely left the cavity.

From Eq. (29) $[\phi_1(z,t) \to \phi(z,T)]$ we find that

$$C_2(t) = \frac{2}{R_k g(t)} \sqrt{\frac{2\varepsilon_0 c \mathcal{A} \eta(T)}{\hbar \omega_k \gamma_{k\mathrm{rad}}}} e^{-i\omega_{23} t} \times \left\{ \frac{\mathrm{d}\phi[c(T-t),T]}{\mathrm{d}t} - i\tilde{\omega}_k^* \phi[c(T-t),T] \right\}. \quad (30)$$

Further, inserting Eq. (19) into Eq. (18) we see that

$$D(t) = f(t) + \int_0^t \mathrm{d}t' f(t) f(t') C_2(t'), \quad (31)$$

where $D(t)$ is defined by

$$D(t) \equiv \dot{C}_2(t) + \frac{R_k^2}{4} \int_0^t \mathrm{d}t' C_2(t') g(t) g(t') e^{-i(\Delta_k - i\Gamma_k/2)(t-t')}, \quad (32)$$

and $f(t)$ is related to the shape of the pump pulse $\Omega_p(t)$ according to

$$f(t) = \frac{i}{2} \Omega_p(t) e^{-i\Delta_p t}. \quad (33)$$

Differentiation of Eq. (31) with respect to t then yields the following differential equation for $f(t)$:

$$D(t)\dot{f}(t) + C_2(t) f^3(t) - \dot{D}(t) f(t) = 0. \quad (34)$$

Hence, the following scheme of shape controlling may be established. For a chosen (i.e., desired) spatiotemporal shape $\phi(z,T)$ of the single-photon outgoing wave packet, the probability amplitude $C_2(t)$ is calculated from Eq. (30). The result is then, together with Eq. (32), inserted into the differential equation (34). Its solution eventually yields the sought shape of the driving pulse.

To illustrate the scheme, we apply it first to the generation of single-photon double-peak wave packets in the case, when the emitter–cavity interaction is constant, as shown in Fig. 6 for two one-photon Fock state generation efficiencies. In the case of low efficiency the shape of the single-photon outgoing wave packet is seen to closely follow the shape of the driving pulse. It is also seen that when an efficiency close to unity is required, then the second peak of the driving pulse must be higher than that

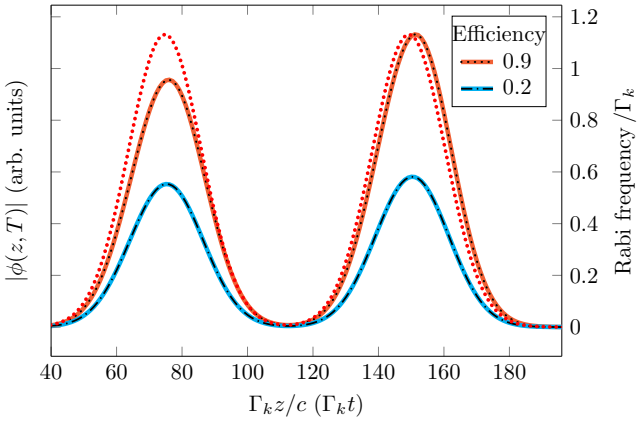

FIG. 6: Shapes of the driving pulse (solid lines) required to generate a double-peak wave packet carrying a one-photon Fock state (dotted red line) for a high generation efficiency $\eta(T) = 0.9$ (solid red line) and a low generation efficiency $\eta(T) = 0.2$ (solid blue line), $R_k = 8\Gamma_k$, $\Delta_k = \Delta_p = 0$, $T = 200\Gamma_k$.

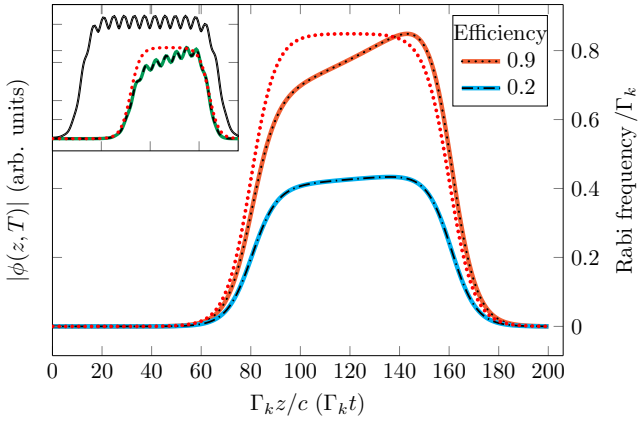

FIG. 7: Shapes of the driving pulse (solid lines) required to generate a plateau-like wave packet carrying a one-photon Fock state (dotted red line) for a high generation efficiency $\eta(T) = 0.9$ (solid red line) and a low generation efficiency $\eta(T) = 0.2$ (solid blue line), $R_k = 8\Gamma_k$, $\Delta_k = \Delta_p = 0$, $T = 200\Gamma_k$. The inset shows the required shape of the driving pulse (solid green line) in the case of a time-dependent shape of the emitter–cavity interaction (solid black line).

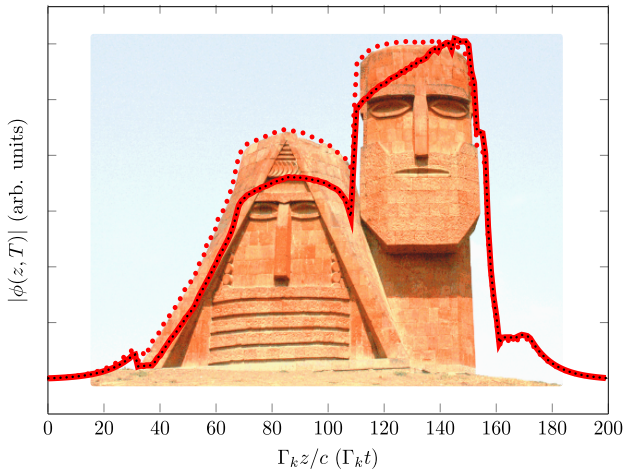

FIG. 8: Shape of the driving pulse (solid red line) required to generate single-photon outgoing wave packets whose shape (dotted red line) resembles the "Tatik-Papik" monument.

of the first one. This can be explained by the fact that during the generation of a single-photon wave packet, a part of the wave packet (which corresponds to the first peak) already escapes the cavity. Therefore, to generate the second required peak the pump intensity should be higher.

A similar behavior is observed in the case when a plateau-like spatiotemporal shape of the single-photon wave packet is desired. as it can be seen from Fig. 7. Namely, in the case of constant emitter–cavity interaction, for low efficiencies the required profile of the driving pulse is similar to the spatiotemporal shape of the outgoing radiation. For generation efficiencies close to unity, the shape of the driving pulse needs to be asymmetric. For comparison, a case of time-dependent emitter–cavity interaction is shown in the inset of Fig. 7. In particular, the interaction shape is chosen to simulate time-dependent variation of the location of the emitter in the cavity, as small oscillations of the interaction due to the variation of emitter position around the anti-nodes of the cavity mode. It is seen that to obtain the desired shape of the single-photon outgoing wave packet, the profile of the driving pulse should follow the variation of the emitter–cavity interaction. Let us finally have a look at Fig. 8. It shows the generation of an asymmetric two-peak wave packet the shape of which resembles the monument called "Tatik-Papik" ("Grandma-Grandpa").

V. SUMMARY AND CONCLUDING REMARKS

Based on macroscopic QED in dispersing and absorbing media, we have presented an exact description of the resonant interaction of a three-level Λ-type emitter in a high-Q cavity with the cavity-assisted electromagnetic field. In particular, we have studied the case when one transition of the emitter resonantly interacts with the cavity field and the other one is subjected to an external classical pump field. We have applied the theory to determine both the efficiency of one-photon Fock state generation and the spatiotemporal shape of the outgoing wave packet. In this context, we have shown that, even for high one-photon Fock state generation efficiencies, wave packets of arbitrary desired shape can be generated by appropriately adjusting the pump.

Under the assumption that the Hilbert space of the total system is spanned by a single-quantum excitation, the quantum state of the excited outgoing nonmonochromatic mode is always a mixture of a one-photon Fock

state and the vacuum state. Due to the unavoidable existence of unwanted losses, such as absorption or scattering, the efficiency of one-photon Fock state generation is always limited by the ratio of the cavity radiative decay rate to the total decay rate, which includes both wanted and unwanted losses.

The spatiotemporal shape of the excited outgoing wave packet and the efficiency of one-photon Fock state generation depend on the interplay of various parameters of the emitter–cavity and emitter–pump interactions, such as their strengths and shapes. In particular, in the case of the vSTIRAP the efficiency of one-photon Fock state generation may be close to the upper limit determined by the unavoidable unwanted losses in the system. It requires that the process is adiabatic and the emitter–cavity interaction is well-established before the driving pulse is applied—so that the system dynamics follows the dark state. However, in this regime, control of the spatiotemporal shape of the excited outgoing wave packet is not possible, as the shape is nearly independent of the driving pulse shape.

In the case when the emitter-cavity interaction can be regarded as being time independent on the timescales of the cavity decay time and the driving pulse length, two interaction regimes may be identified. In the regime when the emitter–cavity interaction Rabi frequency is sufficiently high compared to the (maximum) emitter–pump interaction Rabi frequency, the spatiotemporal shape of the excited outgoing wave packet follows the shape of the driving pulse. However, the one-photon Fock state generation efficiency is very low. This interaction regime has been realized by means of the interaction of a high-finesse cavity with both neutral atoms [11] and trapped ions [12], where single-photon wave packet shapes that follow the driving field shapes have been reported. In the regime when the emitter–pump interaction Rabi frequency is of the same order of magnitude as the emitter–cavity Rabi frequency, the one-photon Fock state generation efficiency is close to the upper limit. However, the spatiotemporal shape of the associated outgoing wave packet has a single-peak profile and is independent on the driving pulse profile.

Desired shapes of outgoing wave packet with high efficiency of one-photon Fock state can be generated by appropriately adjusting the emitter–pump interaction for given emitter–cavity interaction. Since the spatiotemporal shape of the wave packet is robust against fluctuations of the pump pulse, the results found imply the feasibility to produce identical wave packets of desired shape carrying a one-photon Fock state each. As an illustration of the scheme, we have considered the generation of a single-photon double-peak wave packet. In fact, the one-photon Fock state is equally distributed among two time-(space-)separated single-peak wave packets, which is a realization of a time-bin entanglement that can be used to perform quantum key distribution [21]. Importantly, the scheme also allows an optimization of the pump pulse profile to match with specific characteristics of the time dependence of the emitter–cavity interaction, such as injecting the emitter into the cavity or fluctuating emitter motion around the center of the interaction region.

Acknowledgments

M. K. acknowledges valuable discussions with J. Wiersig.

Appendix A: Green tensor

The Green tensor has the following property:

$$\frac{\omega^2}{c^2}\int \mathrm{d}x\, \varepsilon''(x,\omega) G(z_1,x,\omega) G^*(z_2,x,\omega) = \mathrm{Im}\, G(z_1,z_2,\omega). \tag{A1}$$

The Green tensors $G(z_A,z_A,\omega)$ and $G(0^+,z_A,\omega)$ read (see, Ref. [15])

$$G(z_A,z_A,\omega) = -\sum_k \frac{c^2}{\tilde{\omega}_k l}\frac{1}{\omega-\tilde{\omega}_k}\sin^2(\omega_k z_A/c) \tag{A2}$$

and

$$G(0^+,z_A,\omega) = -\sum_k \frac{t_{13}c^2}{2\tilde{\omega}_k l}\frac{i}{\omega-\tilde{\omega}_k} e^{i\omega_k l/c}\sin(\omega_k z_A/c), \tag{A3}$$

respectively, where t_{13} denotes the transmission coefficient from inside the cavity to outside.

Appendix B: Quantum State of the Outgoing field

To calculate the quantum state of the outgoing field, following Ref. [15], we start from the one-dimensional version of Eq. (9) and decompose the electric field into incoming and outgoing fields. Then, we may represent the outgoing field at the point $z=0$ outside the cavity as

$$\underline{\hat{E}}_{\mathrm{out}}(z,\omega)\big|_{z=0^+} = i\sqrt{\frac{\hbar}{\varepsilon_0\pi\mathcal{A}}}\,\frac{\omega^2}{c^2} \times \int \mathrm{d}z' \sqrt{\varepsilon''(z',\omega)}\, G_{\mathrm{out}}(0^+,z',\omega)\hat{f}(z',\omega). \tag{B1}$$

It is useful to introduce the bosonic operators

$$\hat{b}_{\mathrm{out}}(\omega) = 2\sqrt{\frac{\varepsilon_0 c\pi\mathcal{A}}{\hbar\omega}}\;\underline{\hat{E}}_{\mathrm{out}}(z,\omega)\Big|_{z=0^+}, \tag{B2}$$

where

$$\left[\hat{b}_{\mathrm{out}}(\omega), \hat{b}^\dagger_{\mathrm{out}}(\omega')\right] = \delta(\omega-\omega'). \tag{B3}$$

To calculate the quantum state of the outgoing field, we start from the multimode characteristic functional

$$C_{\mathrm{out}}[\beta(\omega),t] = \langle\psi(t)|\exp\left[\int_0^\infty \mathrm{d}\omega\,\beta(\omega)\hat{b}^\dagger_{\mathrm{out}}(\omega) - \mathrm{H.c.}\right]|\psi(t)\rangle\,. \tag{B4}$$

To evaluate $C_{\rm out}[\beta(\omega),t]$ for the state $|\psi(t)\rangle$ as given by Eq. (12), we first note that from Eq. (12) together with the relation $\hat{f}(z,\omega)|\{0\}\rangle = 0$ it follows that

$$\hat{f}(z,\omega)|\psi(t)\rangle = C_3(z,\omega,t)e^{-i(\omega+\omega_{31})t}\ |\{0\}\rangle|3\rangle. \quad \text{(B5)}$$

Hence, on recalling Eqs. (B1) and (B2), it can be seen that

$$\hat{b}_{\rm out}(\omega)|\psi(t)\rangle = F^*(\omega,t)\ |\{0\}\rangle|3\rangle, \quad \text{(B6)}$$

where

$$F(\omega,t) = -2i\sqrt{\frac{c}{\omega}}\frac{\omega^2}{c^2}e^{i(\omega+\omega_{31})t} \times \int \mathrm{d}z\,\sqrt{\varepsilon''(z,\omega)}\,G^*_{\rm out}(0^+,z,\omega)C^*_3(z,\omega,t). \quad \text{(B7)}$$

To represent $C_{\rm out}[\beta(\omega),t]$ in a more transparent form, we introduce a time-dependent unitary transformation according to

$$\beta(\omega) = \sum_i F_i^*(\omega,t)\beta_i(t), \quad \text{(B8)}$$

$$\beta_i(t) = \int_0^\infty \mathrm{d}\omega F_i(\omega,t)\beta(\omega). \quad \text{(B9)}$$

Here, the normalized complex functions $F_i(\omega,t)$ represent nonmonochromatic modes of appropriately chosen frequency distributions where associated nonmonochromatic mode operators read

$$\hat{b}_{{\rm out}\,i}(t) = \int_0^\infty \mathrm{d}\omega\, F_i(\omega,t)\hat{b}_{\rm out}(\omega). \quad \text{(B10)}$$

Note that

$$\hat{b}_{\rm out}(\omega) = \sum_i F_i^*(\omega,t)\hat{b}_{{\rm out}\,i}(t). \quad \text{(B11)}$$

Accordingly, applying the Baker-Campberll-Hausdorf formula, using the commutation relation Eq. (B3) together with Eq. (B6) we may rewrite $C_{\rm out}[\beta(\omega),t]$, Eq. (B4) as

$$C_{\rm out}[\beta_i(t),t] = \exp\left[-\tfrac{1}{2}\sum_i|\beta_i(t)|^2\right] \times \left[1-\left|\sum_i\beta_i(t)\int_0^\infty \mathrm{d}\omega\,F_i(\omega,t)F(\omega,t)\right|^2\right]. \quad \text{(B12)}$$

We now choose

$$F_1(\omega,t) = \frac{F(\omega,t)}{\sqrt{\eta(t)}}, \quad \text{(B13)}$$

with $\eta(t)$ being given by Eq. (23). In this way, from Eq. (B12) we obtain $C_{\rm out}[\beta_i(t),t]$ in a 'diagonal' form with respect to the nonmonochromatic modes:

$$C_{\rm out}[\beta_i(t),t] = C_1[\beta_1(t),t]\prod_{i\neq 1}C_i[\beta_i(t),t], \quad \text{(B14)}$$

where

$$C_1(\beta,t) = e^{-|\beta|^2/2}\left[1-\eta(t)|\beta|^2\right] \quad \text{(B15)}$$

and

$$C_i(\beta,t) = e^{-|\beta|^2/2} \quad (i\neq 1). \quad \text{(B16)}$$

The Fourier transform of $C_{\rm out}[\beta_i(t),t]$ with respect to the $\beta_i(t)$ then yields the (multi-mode) Wigner function $W_{\rm out}(\alpha_i,t)$, Eq. (21).

Substitution of the formal solution of Eq. (15) for $C_3(z,\omega,t)$ [with the initial condition $C_3(z,\omega,0)=0$] into Eq. (B7) and the use of Eq. (A1) yields Eq. (24) (for details, see Ref. [15]).

[1] A. Reiserer and G. Rempe, Rev. Mod. Phys. **87**, 1379 (2015).
[2] E. Knill, R. Laflamme, and G. J. Milburn, Nature **409**, 46 (2001).
[3] J. I. Cirac, P. Zoller, H. J. Kimble, and H. Mabuchi, Phys. Rev. Lett. **78**, 3221 (1997).
[4] I. Marcikic, H. de Riedmatten, W. Tittel, V. Scarani, H. Zbinden, and N. Gisin, Phys. Rev. A **66**, 062308 (2002).
[5] C. K. Law and H. J. Kimble, J. Mod. Opt. **44**, 2067 (1997).
[6] K. Bergmann, H. Theuer, and B. W. Shore, Rev. Mod. Phys. **70**, 1003 (1998).
[7] H. P. Specht, J. Bochmann, M. Mücke, B. Weber, E. Figueroa, D. L. Moehring, and G. Rempe, Nat Photon **3**, 469 (2009).
[8] A. Kiraz, M. Atatüre, and A. Imamoğlu, Phys. Rev. A **69**, 032305 (2004).
[9] G. Jaritz and U. Hohenester, Eur. Phys. J. B **82**, 29 (2011).
[10] M. Mücke, J. Bochmann, C. Hahn, A. Neuzner, C. Nölleke, A. Reiserer, G. Rempe, and S. Ritter, Phys. Rev. A **87**, 063805 (2013).
[11] A. Kuhn, M. Hennrich, and G. Rempe, Phys. Rev. Lett. **89**, 067901 (2002).
[12] M. Keller, B. Lange, K. Hayasaka, W. Lange, and H. Walther, Nature **431**, 1075 (2004).
[13] G. S. Vasilev, D. Ljunggren, and A. Kuhn, New Journal of Physics **12**, 063024 (2010).
[14] P. B. R. Nisbet-Jones, J. Dilley, D. Ljunggren, and A. Kuhn, New J. Phys. **13**, 103036 (2011).
[15] M. Khanbekyan, D.-G. Welsch, C. Di Fidio, and W. Vogel, Phys. Rev. A **78**, 013822 (2008).
[16] C. Di Fidio, W. Vogel, M. Khanbekyan, and D.-G. Welsch, Phys. Rev. A **77**, 043822 (2008).
[17] L. Knöll, S. Scheel, and D.-G. Welsch, *Coherence and*

Statistics of Photons and Atoms (Wiley, New York, 2001), p. 1, quant-ph/0003121.

[18] W. Vogel and D.-G. Welsch, *Quantum Optics* (Wiley-VCH, Weinheim, 2006), 3rd ed.

[19] A. S. Parkins, P. Marte, P. Zoller, and H. J. Kimble, Phys. Rev. Lett. **71**, 3095 (1993).

[20] C. K. Law and J. H. Eberly, Phys. Rev. Lett. **76**, 1055 (1996).

[21] W. Tittel, J. Brendel, H. Zbinden, and N. Gisin, Phys. Rev. Lett. **84**, 4737 (2000).